

Examining the Limitations of Dynamic Mode Decomposition through Koopman Theory Analysis*

Ido Cohen[†] and Guy Gilboa[†]

Abstract. This work binds the existence of *Koopman Eigenfunction* (KEF), the geometric of the dynamics, and the validity of *Dynamic Mode Decomposition* (DMD) to one coherent theory. Viewing the dynamic as a curve in the state-space allows us to formulate an existence condition of KEFs and their multiplicities. These conditions lay the foundations for system reconstruction, global controllability, and observability for nonlinear dynamics.

DMD can be interpreted as a finite dimension approximation of *Koopman Mode Decomposition* (KMD). However, this method is limited to the case when KEFs are linear combinations of the observations. We examine the limitations of DMD through the analysis of Koopman theory. We propose a new mode decomposition technique based on the typical time profile of the dynamics. An overcomplete dictionary of decay profiles is used to sparsely represent the dynamic. This analysis is also valid in the full continuous setting of Koopman theory, which is based on variational calculus. We demonstrate applications of this analysis, such as finding KEFs and their multiplicities, calculating KMD, dynamics reconstruction, global linearization, and controllability.

Key words. nonlinear decomposition, dynamic mode decomposition, homogeneous operators, gradient flows, nonlinear spectral theory, Koopman eigenfunctions, Koopman mode decomposition.

1. Introduction. Knowing the latent space of certain data allows one to represent it concisely and differentiate between fine signal and clutter parts. Recovering this space in a data-driven manner is a long-standing research problem. Data resulting from dynamical systems is represented commonly as spatial structures (modes) that are attenuated or enhanced with time. The Koopman theory argues that there are data measurements that evolve as if the dynamical system is linear. A well-known algorithm to approximate these measurements is DMD [45], proposed by Schmid. In this work, we formulate sufficient and necessary conditions for the existence of these measurements. These findings highlight certain flaws of DMD. Finally, we suggest a new mode decomposition to overcome some of these problems, originated in general spectral decomposition [24].

In many dynamical processes, there are measurements of the observations that evolve linearly, or approximately so [41]. A theoretical justification for that can be traced back to the seminal work of Bernard Osgood Koopman in 1931 [29]. These measurements are referred to as KEFs. In [39] an algorithm was proposed, KMD, which aims to reconstruct the dynamics using spatial structures, termed as modes, which are the coefficients of Koopman eigenfunctions. Since KEFs evolve as if they were observations in a linear dynamical system, KMD can interpret the original dynamics as a linear one.

This decomposition might be infinite-dimensional. An approximation of KMD, in a finite

*

Funding: This work was supported by the European Union's Horizon 2020 research and innovation programme under the Marie Skłodowska-Curie grant agreement No. 777826 (NoMADS). GG acknowledges support by the Israel Science Foundation (Grant No. 534/19) and by the Ollendorff Minerva Center.

[†]Electrical Engineering Department at the Technion – Israel Institute of Technology (ido@campus.technion.ac.il, guy.gilboa@ee.technion.ac.il).

domain, was suggested in [45] named DMD. If the KEFs measurements are linear combinations of the observations DMD yields the Koopman mode accurately [45]. As noted in [31], DMD can be interpreted as exponential data fitting algorithm. In the more general nonlinear case, DMD may not reveal well the underlying modes and dynamics.

Recently the authors and colleagues have formalized this insight in [13], in the context of homogeneous flows, referring to it as the DMD paradox. As the step-size approaches zero, dynamic reconstruction with DMD results in positive mean squared error but, paradoxically, with zero DMD error. In general, this paradox exists in any dynamical system whose KEFs are not linear combinations of the observations. This phenomenon becomes extreme when the system is zero homogeneous [14]. In that case, the dynamics is only in C^0 almost everywhere and exponential decay is a very crude and inaccurate approximation. In such cases, lifting the observations to a finite higher dimensional space does not solve the problem (see for example [30, 50]).

This alleged contradiction between KMD and DMD leads us to examine the fundamentals of Koopman theory. We follow the general solution of the KEF concerning time and analyze the mapping from the state-space back to the time variable. The existence of this mapping depends on the smoothness condition of the dynamics. After formulating the existence condition of KEFs, KMD becomes easy to calculate. As a direct result, we introduce a new method that overcomes the DMD limitations. These findings, with some adaptations, are valid in the full continuous settings, discussed [32, 37].

Main Contributions. We formulate the conditions for the existence of a KEF. If it exists, there is an infinite set of KEFs. We distinguish between different types of eigenfunction groups and analyze their multiplicity. We show that certain multiplicities are crucial to obtain dynamics reconstruction, controllability, and observability (Sec. 3). These conclusions are extended to the full continuous setting. Conditions for the existence of *Koopman Eigenfunctionals* (KEFals) are presented (Sec. 4). Following these insights, we suggest an alternative algorithm for finding Koopman modes induced by fitting time functions that best characterize the dynamics. This algorithm overcomes some inherent limitations of DMD (Sec. 5). Throughout this work, we illustrate the theory with simple toy examples. Additional examples and experiments are given in Sec. 6. In the following section, we provide the essential definitions and notations.

2. Preliminary. In this section, we provide notations and background on Koopman operators, eigenfunctions and eigenfunctionals, DMD and some properties in variational calculus (relevant to Sec. 4). In addition, we outline the work of Katzir & Gilboa [24, 27], where nonlinear flows emerging in signal and image-processing are decomposed through a dictionary of decay profiles. We adapt this method for the extraction of Koopman modes in Sec. 5.

2.1. Koopman theory.

2.1.1. Discrete spatial setting. We consider a dynamical system in a semi-discrete setting of the form of,

$$(2.1) \quad \frac{d}{dt} \mathbf{x}(t) = P(\mathbf{x}(t)), \quad \mathbf{x}(0) = \mathbf{x}_0, \quad t \in I,$$

where $\mathbf{x} \in \mathbb{R}^N$ is state vector, $P : \mathbb{R}^N \rightarrow \mathbb{R}^N$ is a (nonlinear) operator, and $I = [a, b] \subseteq \mathbb{R}^+$ is a time interval. Let $g : \mathbb{R}^N \rightarrow \mathbb{R}$ be a measurement of \mathbf{x} . The Koopman operator K_P^τ is defined by [29, 39],

$$(KO) \quad K_P^\tau(g(\mathbf{x}(s))) = g(\mathbf{x}(s + \tau)), \quad s, s + \tau \in I,$$

where $\tau > 0$. The Koopman operator is linear, namely it admits,

$$K_P^\tau(g(\mathbf{x}(s)) + f(\mathbf{x}(s))) = K_P^\tau(g(\mathbf{x}(s))) + K_P^\tau(f(\mathbf{x}(s))),$$

for all measurements g and f . In addition, the Koopman operators $\{K_P^\tau\}_{\tau \geq 0}$ is a semigroup of operators, more formally,

$$K_P^{\tau_2} \circ K_P^{\tau_1} = K_P^{\tau_1 + \tau_2},$$

where \circ denotes the composition operator.

An eigenfunction of the Koopman operator, $\varphi(\mathbf{x})$, admits,

$$(2.2) \quad K_P^\tau(\varphi(\mathbf{x}(s))) = \varphi(\mathbf{x}(s + \tau)) = \eta^\tau \varphi(\mathbf{x}(s)), \quad s, s + \tau \in I.$$

Due to the semigroup attribute of the Koopman operator, the following limit exists,

$$(2.3) \quad \lim_{\tau \rightarrow 0} \frac{K_P^\tau(\varphi(\mathbf{x}(s))) - \varphi(\mathbf{x}(s))}{\tau} = \lim_{\tau \rightarrow 0} \frac{\varphi(\mathbf{x}(s + \tau)) - \varphi(\mathbf{x}(s))}{\tau} = \left. \frac{d}{dt} \varphi(\mathbf{x}(t)) \right|_{t=s}.$$

It can be shown (see for instance [38], p. 10) that a KEF admits,

$$(2.4) \quad \frac{d}{dt} \varphi(\mathbf{x}(t)) = \lambda \cdot \varphi(\mathbf{x}(t)), \quad \forall t \in I,$$

where $\eta = e^\lambda$ and $\lambda \in \mathbb{C}$. This limit can be explained by the relations of the Koopman operator and Lie derivatives [6]. The solution of this linear ODE is given by

$$(KEF) \quad \varphi(\mathbf{x}(t)) = \varphi(\mathbf{x}(a)) e^{\lambda t}, \quad \forall t \in I.$$

2.1.2. Full continuous setting. Let $u : L \subset \mathbb{R} \times I \subseteq \mathbb{R}^+$ be the solution of the following PDE,

$$(2.5) \quad u_t(x, t) = \mathcal{P}(u(x, t)), \quad u(x, 0) = f(x).$$

We assume that u belongs to a Hilbert space \mathcal{H} with an inner product, $\langle v, u \rangle$ and its associated norm $\|\cdot\| = \sqrt{\langle \cdot, \cdot \rangle}$, $\mathcal{P} : \mathcal{H} \rightarrow \mathcal{H}$ is a (nonlinear) operator. Let $Q : \mathcal{H} \rightarrow \mathbb{R}$ be a proper, lower-semicontinuous functional. The Koopman operator, K_P^τ , in the sense of PDE, is defined by,

$$(2.6) \quad K_P^\tau(Q(u(x, s))) = Q(u(x, s + \tau)), \quad s, s + \tau \in I.$$

An eigenfunctional, ϕ , of the Koopman operator is a functional admitting the following,

$$(2.7) \quad K_P^\tau(\phi(u(x, s))) = \phi(u(x, s + \tau)) = \eta^\tau \phi(u(x, s)), \quad s, s + \tau \in I.$$

By letting $\tau \rightarrow 0$ an eigenfunctional of the Koopman operator admits the following ODE,

$$(2.8) \quad \frac{d}{dt} \phi(u(x, t)) = \lambda \phi(u(x, t)),$$

where $\eta = e^\lambda$. Thus, a *Koopman Eigenfunctional* (KEFal) is of the form,

$$(KEFal) \quad \phi(u(x, t)) = \phi(u(x, a)) e^{\lambda t}, \quad \forall t \in I.$$

2.2. Dynamic Mode Decomposition (DMD). DMD extracts the main spatial structures in the dynamics [45]. Backed by Koopman theory, DMD is a principal method to approximate the Koopman modes. It is a data driven method, based on snapshots of the dynamics. The main steps in DMD and its extensions (e.g. Exact DMD[46] tIsDMD[25] fbDMD[18] S-DMD[13] and optimized DMD [1]) are:

1. *Coordinates representation* - finding the main structures in the dynamics.
2. *Dimensionality reduction* - choosing the dominant parts of the dynamics.
3. *Linear mapping* - finding a linear mapping in the reduced dimensional space (see [45] Eq. 2.2).

We describe these steps in detail in Appendix A. DMD is data drive algorithm, based on the samples of the solution $\mathbf{x}_k = \mathbf{x}(t_k)$. Mostly, the solution is sampled uniformly in time. The result of DMD and its variants is a set of *modes*, $\{\phi_i\}$, *eigenvalues* $\{\mu_i\}$, and *coefficients* $\{\alpha_i\}$, where $i = 1, \dots, r$ and r is the reduced dimension. They can be used to reconstruct an approximation of the dynamics by,

$$(2.9) \quad \tilde{\mathbf{x}}_k \approx \sum_{i=1}^r \alpha_i \mu_i^k \phi_i.$$

2.3. General Spectral Decomposition. One of the main goals of signal analysis is to represent a signal sparsely and yet precisely. To achieve this goal there are many applications and methods. Decomposing signals through PDE analysis often involves the approximated solution (2.5) formulated as,

$$(2.10) \quad u(x, t) \approx \sum_{i=1}^L h_i(x) a_i(t),$$

where $\{h_i(\cdot)\}_{i=1}^L$ are spatial functions and their respectively attenuating or enhancing functions are $\{a_i(t)\}_{i=1}^L$. The time functions are usually typical to the operator \mathcal{P} [15].

This insight can be applied also on the semi-discrete setting system. Then, the solution of Eq. (2.1) can be formulated as

$$(2.11) \quad \mathbf{x}(t) \approx \sum_{i=1}^L \mathbf{v}_i a_i(t)$$

where the $\{\mathbf{v}_i\}_{i=1}^L$ are the spatial structures and $\{a_i(t)\}_{i=1}^L$ are the corresponding time functions. Note that in some cases (e.g. linear diffusion or *Total Variation* (TV) flow [10]) Eqs. (2.10) and (2.11) achieve equality for finite or infinite L .

This is the basis of the general spectral decomposition suggested by Katzir & Gilboa in [24, 27]. The initial condition of Eq. (2.5) is reconstructed with spatial structures that decay according to a known time function. More formally, given the solution, $u(x, t)$, we solve the following optimization problem

$$(2.12) \quad \|\mathcal{U} - \mathcal{HD}\|_F^2$$

where \mathcal{U} is a matrix of the sampled solution in the time and space domains, \mathcal{H} is a matrix which its columns are the main spatial structures, and \mathcal{D} is a dictionary of decay profiles. More formally, we can write them as

$$(2.13) \quad \mathcal{U} = \begin{bmatrix} u(x_1, t_0) & \cdots & u(x_1, t_M) \\ \vdots & & \vdots \\ u(x_N, t_0) & \cdots & u(x_N, t_M) \end{bmatrix}, \mathcal{H} = \begin{bmatrix} h_1(x_1) & \cdots & h_r(x_1) \\ \vdots & & \vdots \\ h_1(x_N) & \cdots & h_r(x_N) \end{bmatrix}, \mathcal{D} = \begin{bmatrix} a_1(t_0) & \cdots & a_1(t_M) \\ \vdots & & \vdots \\ a_r(t_0) & \cdots & a_r(t_M) \end{bmatrix},$$

where $\mathcal{U} \in \mathbb{R}^{N \times (M+1)}$, $\mathcal{H} \in \mathbb{R}^{N \times r}$, and $\mathcal{D} \in \mathbb{R}^{r \times (M+1)}$. The optimization problem, Eq. (2.12), fits also the form of semi-discrete setting in the dynamics Eq. (2.1) where it is sampled in the time axis. Then, we can formulate the following optimization problem

$$(2.14) \quad \|X - \mathcal{V}\mathcal{D}\|_{\mathcal{F}}^2$$

where the matrix X contains the samples of the dynamics

$$(2.15) \quad X = [\mathbf{x}_0 \quad \mathbf{x}_1 \quad \cdots \quad \mathbf{x}_M] \in \mathbb{R}^{N \times (M+1)},$$

the matrix \mathcal{V} contains the main spatial structure of the dynamic (Eq. (2.11))

$$(2.16) \quad \mathcal{V} = [\mathbf{v}_1 \quad \mathbf{v}_2 \quad \cdots \quad \mathbf{v}_r] \in \mathbb{R}^{N \times r},$$

and the dictionary, \mathcal{D} , remains unchanged.

This decomposition generalizes the decomposition based on gradient descent flow analysis of a γ -homogeneous functional where $\gamma \in [1, 2)$ [9, 10, 16, 22, 23]. The flow is formulated as a PDE of the form of Eq. (2.5) where \mathcal{P} is a $(\gamma - 1)$ -homogeneous operator. Under these flows, spatial structures remain unchanged and decay in a typical profile to the homogeneity.

2.4. Variational Calculus.

Brezis chain rule. The time derivative of a functional can be expressed through the ‘‘chain rule’’ of Brezis [4] as,

$$(2.17) \quad \frac{d}{dt}Q(u(x, t)) = \langle \partial_u Q, \frac{d}{dt}u(x, t) \rangle = \langle \partial_u Q, \mathcal{P}(u(x, t)) \rangle,$$

where $\partial_u Q$ is the variational derivative of the functional Q .

Fréchet Differentiability. The operator $\mathcal{P} : \mathcal{H} \rightarrow \mathcal{H}$ is Fréchet differentiable at u if there exists a bounded linear operator \mathcal{L} , such that,

$$(2.18) \quad \lim_{\|h\| \rightarrow 0} \frac{\|\mathcal{P}(u+h) - \mathcal{P}(u) - \mathcal{L}(h)\|}{\|h\|} = 0$$

holds from any $h \in \mathcal{H}$. In this case, $\mathcal{P}(u+h)$ can be expanded in the Landau notation as

$$(2.19) \quad \mathcal{P}(u+h) = \mathcal{P}(u) + \mathcal{L}(h) + o(h),$$

where $\lim_{\|h\| \rightarrow 0} \|o(h)\|/\|h\| = 0$.

Proper Operator. The operator $\mathcal{P}(f(x))$ is proper if it gets a finite value for any $f(x) \in \mathcal{H}$ and for any $x \in [0, L]$.

Region of Attraction (ROA). Let \mathbf{x}^* be an equilibrium point of the dynamical system in Eq. (2.1). The region of attraction is the largest set in \mathbb{R}^N that admits the following property: if the initial condition of the dynamics is from the set, then the system converges to \mathbf{x}^* (see e.g. [47]). More formally,

$$(2.20) \quad \mathcal{RA}(\mathbf{x}^*) = \{x_{init} \in \mathbb{R}^N | \mathbf{x}(t=0) = x_{init}, \lim_{t \rightarrow \infty} \mathbf{x}(t) = \mathbf{x}^*\}.$$

3. Koopman Eigenfunctions and Modes. Koopman theory provides linear representation to data that emerges from nonlinear systems. These representations are based on measurements in the state-space termed as *Koopman eigenfunctions*. Necessary and sufficient conditions for their existence are formulated here. Since the eigenfunctions are not unique, we define the *Koopman family*, an infinite set of Koopman eigenfunctions. We also define a useful notion, referred to as the *ancestors of a Koopman family*. This allows the reconstruction of the dynamical system, under certain conditions. Moreover, it allows to considerably enlarge the *Region of Attraction* (ROA) of the system. The above conclusions are consequences of the attributes of the dynamics, P , and its solution, $\mathbf{x}(t)$, discussed and analyzed below.

3.1. Koopman Eigenfunctions. We first set the necessary degree of smoothness of P , required to develop the theory. This setting is highly non-restrictive and accommodates most useful linear and nonlinear dynamics. We refer to the operator P in the dynamical system (2.1).

Assumption 3.1 (Piecewise Continuous P). *The operator $P : \mathbb{R}^N \rightarrow \mathbb{R}^N$ is in C^0 a.e. with zero Dirac measures.*

This leads to the following Lemma.

Lemma 3.2 (Continuous solution $\mathbf{x}(t)$). *If the operator P in Eq. (2.1) admits Assumption 3.1 then the solution, \mathbf{x} , is in C^1 a.e.*

Proof. The solution of the dynamics is

$$(3.1) \quad \mathbf{x}(t) = \mathbf{x}(a) + \int_a^t P(\mathbf{x}(\tau)) d\tau.$$

The solution, $\mathbf{x}(t) \in C^1$ a.e. since $P \in C^0$ a.e. and does not contain Dirac measures. ■

The solution, $\mathbf{x}(t)$, $t \in I \subset \mathbb{R}^+$, maps from I to \mathbb{R}^N . It can be interpreted as a parametric curve in \mathbb{R}^N , where its tangential velocity is $P(\mathbf{x})$. Let us denote the image of $\mathbf{x}(t)$ as \mathcal{X} . The image is the path in \mathbb{R}^N where the system passes along the interval I . We note that Lemma 3.2 holds also if Assumption 3.1 is limited to \mathcal{X} .

A Koopman eigenfunction is a measurement of the solution \mathbf{x} that admits Eq. (2.4) on the curve \mathcal{X} . As recently was stated in [3], a Koopman eigenfunction can be formulated as an exponential function, where its argument is the inverse mapping from \mathcal{X} to I . The formal definition of the mapping is as follows.

Definition 3.3 (Time state-space mapping). Let $\mathbf{x}(t)$ be the solution of the dynamical system (2.1) where $t \in I$. Let $\xi : \mathcal{X} \rightarrow I$ be a time state-space mapping from \mathbf{x} to t ,

$$(3.2) \quad t = \xi(\mathbf{x}).$$

This mapping is possible if the curve \mathcal{X} is simple and open. Necessary conditions of a curve to be simple are discussed, for instance, in [12] and the references therein.

Lemma 3.4 (Differentiation of time state-space mapping). Let the conditions of Lemma 3.2 hold. If the time state-space mapping, $t = \xi(\mathbf{x})$, exists then it admits the following,

$$(3.3) \quad \nabla \xi(\mathbf{x})^T P(\mathbf{x}) = 1 \quad \text{a.e. in } \mathcal{X}.$$

Proof. The mapping $\xi(\mathbf{x})$ is in C^1 a.e. in \mathcal{X} since $\mathbf{x}(t) \in C^1$ a.e. in I . The time derivative of the mapping is,

$$(3.4) \quad 1 = \frac{d}{dt}t = \frac{d}{dt}\xi(\mathbf{x}) = \nabla \xi(\mathbf{x})^T \frac{d}{dt}\mathbf{x} = \nabla \xi(\mathbf{x})^T P(\mathbf{x}).$$

This expression is valid almost everywhere. ■

We now turn to discuss necessary and sufficient conditions for the existence of a nontrivial Koopman eigenfunction (that is, a nonzero function which admits Eq. (2.4) with $\lambda \neq 0$).

Proposition 3.5 (Condition for the inexistence of a Koopman eigenfunction). If there is an equilibrium point in I then a nontrivial Koopman eigenfunction does not exist.

Proof. Let $t_0 \in I$ be an equilibrium point and $\varphi(\mathbf{x}(t))$ be a Koopman eigenfunction. Then, $\mathbf{x}(t) = \text{const}$, $\forall t \in [t_0, b]$. Therefore, Eq. (2.4) does not hold for nontrivial φ for any $\lambda \neq 0$. ■

Remark 3.6 (Finite Support Time Dynamics). Let $P(\mathbf{x})$ define a dynamic for which the solution has a finite support in time. Namely, there is an extinction time point, T_{ext} , for which $P(\mathbf{x}(t)) = \mathbf{0}$, $\forall t \geq T_{ext}$. Then, if $T_{ext} \in I$, a Koopman operator K_P^T has no eigenfunctions. We observe here that the time interval I is crucial for the existence or inexistence of eigenfunctions.

From a differential geometry perspective, as noted above, $\mathbf{x}(t)$ forms a curve where its tangential velocity is $P(\mathbf{x})$. The absence of an equilibrium point is equivalent to nonzero velocity. This type of parametric curves, where the velocity is always nonzero, is called *regular*. The Koopman eigenfunction does not exist for non-regular curves. Note that a discussion on equilibrium points is conducted in [5], in the context of DMD and its variants.

Lemma 3.7 (Koopman Eigenfunctions induced by a Time State-Space Mapping). Let the conditions of Lemma 3.2 hold and $\mathbf{x}(t)$ be the solution of Eq. (2.1). If there exists a time state-space mapping, $t = \xi(\mathbf{x})$, then a Koopman eigenfunction exists.

Proof. The mapping, $t = \xi(\mathbf{x})$, is in C^1 a.e. in \mathcal{X} since $\mathbf{x}(t)$ is in C^1 a.e. in I . Given that mapping, we define the following function,

$$(3.5) \quad \varphi(\mathbf{x}) = e^{\alpha \xi(\mathbf{x}) + \beta}.$$

This function is in C^1 a.e. in \mathcal{X} . The time derivative of this function is,

$$(3.6) \quad \frac{d}{dt}\varphi(\mathbf{x}(t)) = \frac{d}{d\xi}e^{\alpha \xi(\mathbf{x}) + \beta} \nabla \xi(\mathbf{x})^T \frac{d}{dt}\mathbf{x} = \alpha \varphi(\mathbf{x}(t)) \nabla \xi(\mathbf{x})^T P(\mathbf{x}(t)).$$

According to Lemma 3.4, $\nabla \xi(\mathbf{x})^T P(\mathbf{x}(t)) = 1$ a.e.. Thus, the function in Eq. (3.5) admits Eq. (2.4) for any value of β , where the corresponding eigenvalue is $\lambda = \alpha$. ■

Theorem 3.8 (Sufficient condition for the existence of a Koopman eigenfunction). *Let the conditions of Lemma 3.2 hold and one of the entries of the vector $P(\mathbf{x}(t))$ is either positive or negative $\forall t \in I$. Then, Koopman eigenfunctions exist in the time interval I .*

Proof. If one of the entries in $P(\mathbf{x}(t))$ is either positive or negative for all $t \in I$ then this entry is monotone and therefore injective. Then, the curve \mathcal{X} is simple and open (see [17] pages 45, 177 and 207). Therefore, the time state-space mapping, $\xi(\mathbf{x})$, exists. Following Lemma 3.7, Koopman eigenfunctions can be expressed by (3.5). ■

The simple example below illustrates the connections between the equilibrium point, finite time dynamics and time state-space mapping.

EXAMPLE 3.9 (Finite time support). Let us consider the following dynamics,

$$(3.7) \quad \frac{d}{dt}x = -2x^{\frac{1}{2}}, \quad x(0) = 1.$$

The solution is

$$(3.8) \quad x(t) = \begin{cases} (1-t)^2 & t \in [0, 1] \\ 0 & t > 1 \end{cases}.$$

For $I = [0, 1]$, the time state-space mapping is,

$$(3.9) \quad t(x) = 1 - \sqrt{x}, \quad I = [0, 1],$$

and using (3.5) with $\alpha = 1$, $\beta = 1$, we can express a Koopman eigenfunction by,

$$(3.10) \quad \varphi(x) = e^{1-\sqrt{x}}.$$

Now, let us repeat this example with a different time interval. Let $I = [0, 1.5]$, containing the extinction time $T_{ext} = 1$. Note that, first, the time mapping, Eq. (3.9), does not hold in the entire interval, and the eigenfunction φ does not admit $\frac{d}{dt}\varphi(x) = \varphi(x)$ since $\varphi(x)$ is a nonzero constant for $t \in [1, 1.5]$. ■

3.2. Koopman Family. The KEF is of the form $\varphi(t) = e^{\alpha t + \beta}$ (Eq. (3.5)). This form of solution is unique following a standard existence and uniqueness theorem of ODE's. The exponential parameters, α and β , are dictated by the eigenvalue and the initial condition. Without these restrictions, there are infinite KEFs for any dynamical system.

From a different angle, viewing the state-space \mathbf{x} as a curve gives a compelling interpretation of the multiplicity of Koopman eigenfunctions. A curve can be reparameterized in different manners. Changing the parameters, α and β , amounts to reparameterization by translation and scaling. This insight leads us to the following lemma, which extends the identities presented in [3]. We show that any mathematical manipulation on a KEF which maintains the form of Eq. (3.5) generates a new KEF.

Lemma 3.10 (Multiplicities of Koopman eigenfunctions). *If φ_1, φ_2 are Koopman eigenfunctions with the corresponding eigenvalues λ_1, λ_2 then:*

1. The function $a \cdot \varphi_1$, $a \in \mathbb{R}$ ($a \neq 0$) is an eigenfunction with eigenvalue λ_1 .
2. The function $(\varphi_1)^\alpha$, $\alpha \in \mathbb{C}$ ($\alpha \neq 0$) is an eigenfunction with eigenvalue $\alpha\lambda_1$.
3. For any $n, m \in \mathbb{R}$ the function $(\varphi_1)^n (\varphi_2)^m$ is an eigenfunction with eigenvalue $n\lambda_1 + m\lambda_2$.
4. The function $(\varphi_1)^{\frac{\lambda}{\lambda_1}} + (\varphi_2)^{\frac{\lambda}{\lambda_2}}$ is an eigenfunction with eigenvalue λ .

Proof. This can be shown by,

1. From the linearity of the Koopman operator.
2. Writing the time derivative of $(\varphi_1)^n (\varphi_2)^m$ explicitly we get,

$$(3.11) \quad \frac{d}{dt} [\varphi_1^\alpha] = \alpha(\varphi_1)^{\alpha-1} \lambda_1 \varphi_1 = \alpha \lambda_1 \varphi_1^\alpha.$$

3. Similarly,

$$(3.12) \quad \begin{aligned} \frac{d}{dt} [(\varphi_1)^n (\varphi_2)^m] &= (\varphi_2)^m n (\varphi_1)^{n-1} \lambda_1 \varphi_1 + (\varphi_1)^n m (\varphi_2)^{m-1} \lambda_2 \varphi_2 \\ &= (n\lambda_1 + m\lambda_2) (\varphi_1)^n (\varphi_2)^m. \end{aligned}$$

4. Finally,

$$(3.13) \quad \begin{aligned} \frac{d}{dt} \left[(\varphi_1)^{\frac{\lambda}{\lambda_1}} + (\varphi_2)^{\frac{\lambda}{\lambda_2}} \right] &= \frac{\lambda}{\lambda_1} (\varphi_1)^{\frac{\lambda}{\lambda_1}-1} \lambda_1 \varphi_1 + \frac{\lambda}{\lambda_2} (\varphi_2)^{\frac{\lambda}{\lambda_2}-1} \lambda_2 \varphi_2 \\ &= \lambda \left[(\varphi_1)^{\frac{\lambda}{\lambda_1}} + (\varphi_2)^{\frac{\lambda}{\lambda_2}} \right]. \end{aligned} \quad \blacksquare$$

Discussion. The multiplicities presented in Lemma 3.10 are translation and scaling of the time variable. Case 1 in this Lemma is a translation of the time axis and the rest of the cases are scaling. To distinguish between eigenfunctions which are generated from other eigenfunctions and “new” independent ones, we introduce the concepts of *Koopman family* and its *ancestors*.

Definition 3.11 (Koopman family). Let $\{\varphi_i\}_{i=1}^n$ be a finite set of KEFs. Let $k_P(\{\varphi_i\}_{i=1}^n)$ be the infinity uncountable set of KEFs generated by the finite set, recursively, according to the four options in Lemma 3.10. Let us define $k_P^m(\{\varphi_i\}_{i=1}^n) = k_P(k_P^{m-1}(\{\varphi_i\}_{i=1}^n))$. We term $\mathcal{K}_P(\{\varphi_i\}_{i=1}^n) = \cup_{m=1}^{\infty} k_P^m(\{\varphi_i\}_{i=1}^n)$ as the *Koopman family* of $\{\varphi_i\}_{i=1}^n$.

Definition 3.12 (Ancestors of a Koopman family). Let $\{\varphi_i^*\}_{i=1}^m$ be a finite set of KEFs. This set is an ancestor set of the Koopman family $\mathcal{K}_P(\{\varphi_i\}_{i=1}^n)$ if the following conditions hold:

1. $\varphi \in \mathcal{K}_P(\{\varphi_i\}_{i=1}^n) \iff \varphi \in \mathcal{K}_P(\{\varphi_i^*\}_{i=1}^m)$.
2. $\varphi_j^* \notin \mathcal{K}_P(\{\varphi_i^*\}_{i=1, i \neq j}^m)$ for any $j = 1, 2, \dots, m$.

Note that the subscript P is for the dynamical system.

3.2.1. Koopman Eigenfunction Vector. A vector of Koopman eigenfunctions is denoted by,

$$(3.14) \quad \boldsymbol{\varphi}(\mathbf{x}) = [\varphi_1(\mathbf{x}) \quad \dots \quad \varphi_L(\mathbf{x})]^T,$$

where L can be finite or infinite. The Jacobian matrix of this vector is,

$$(3.15) \quad \frac{\partial}{\partial \mathbf{x}} \boldsymbol{\varphi}(\mathbf{x}) = \begin{bmatrix} \nabla \varphi_1(\mathbf{x})^T \\ \vdots \\ \nabla \varphi_L(\mathbf{x})^T \end{bmatrix} = \mathcal{J}(\boldsymbol{\varphi}).$$

Theorem 3.13 (Linear dynamic in Koopman family). *Let the conditions of Theorem 3.8 hold. The dynamical system P can be represented as a linear one with a Koopman eigenfunction vector, where the time derivative of this vector is,*

$$(3.16) \quad \frac{d}{dt} \boldsymbol{\varphi}(\mathbf{x}) = \mathcal{J}(\boldsymbol{\varphi})P(\mathbf{x}) = \Lambda \boldsymbol{\varphi}(\mathbf{x}), \quad a.e.$$

where Λ is a diagonal matrix with the corresponding eigenvalues.

Proof. We would like to prove first the existence of a L dimensional KEF. From Theorem 3.8 there exists a KEF. From Lemma 3.10 if there exists a KEF, there are infinite set of KEFs, therefore, at least L eigenfunctions. According to the definition of the Koopman eigenfunction, the time derivative is,

$$(3.17) \quad \frac{d}{dt} \boldsymbol{\varphi}(\mathbf{x}) = \left[\frac{d}{dt} \varphi_1(\mathbf{x}), \dots, \frac{d}{dt} \varphi_L(\mathbf{x}) \right]^T = \left[\lambda_1 \varphi_1(\mathbf{x}), \dots, \lambda_L \varphi_L(\mathbf{x}) \right]^T = \Lambda \boldsymbol{\varphi}(\mathbf{x}).$$

On the other hand, applying the chain rule we get,

$$(3.18) \quad \frac{d}{dt} \boldsymbol{\varphi}(\mathbf{x}) = \begin{bmatrix} \nabla \varphi_1(\mathbf{x})^T \\ \vdots \\ \nabla \varphi_L(\mathbf{x})^T \end{bmatrix} \frac{d}{dt} \mathbf{x}(t) = \mathcal{J}(\boldsymbol{\varphi})P(\mathbf{x}).$$

Note that $\varphi_i(\mathbf{x}) \in C^1$, (a.e.), so the expressions above are valid only almost everywhere. ■

3.2.2. Reconstructing the dynamics. The ability to reconstruct the dynamics is based on the relations between the vectors $\boldsymbol{\varphi}$ and \mathbf{x} . In classical control theory, this is referred to as *observability*. Here, we suggest to examine the notion of observability by computing the rank of the Jacobian matrix $\mathcal{J}(\boldsymbol{\varphi})$, Eq. (3.15). The rows of this matrix are the gradients of the KEFs. The following lemma shows that the gradient of a member of a Koopman family originates with its ancestors.

Lemma 3.14 (KEF gradients of a family). *Let $\mathcal{K}_P(\{\varphi_i^*\}_{i=1}^m)$ be the Koopman family of an ancestor set, $\{\varphi_i^*\}_{i=1}^m$. Let φ be a KEF in $\mathcal{K}_P(\{\varphi_i^*\}_{i=1}^m)$. Then, the gradient of φ , $\nabla \varphi$, is a linear combination of the gradients of the ancestor set for any $t \in I$.*

Proof. Let $\mathcal{K}\mathcal{G}$ be the linear span, defined by

$$(3.19) \quad \mathcal{K}\mathcal{G} = \text{span}(\{\nabla \varphi_i^*\}_{i=1}^m) = \left\{ \sum_{i=1}^m a_i \nabla \varphi_i^*, \forall a_i \in \mathbb{C} \right\}.$$

Let φ be in $\mathcal{K}_P(\{\varphi_i^*\}_{i=1}^m)$. According to Definition 3.11, there exist recursive steps leading from the ancestors $\{\varphi_i^*\}_{i=1}^m$ to φ . Now, by induction we show that $\nabla \varphi \in \mathcal{K}\mathcal{G}$. Let us assume

that from the ancestors to φ there is one step. Namely, φ is generated using φ_i^*, φ_j^* , according to the four cases of Lemma 3.10. The gradient of φ is a linear combination of the gradients of φ_i^* and φ_j^* . For cases 1, 2 and 4, the linearity is straightforward. For case 3, $\varphi = (\varphi_i^*)^n (\varphi_j^*)^l$, we have,

$$(3.20) \quad \begin{aligned} \nabla\varphi &= \nabla(\varphi_i^*)^n (\varphi_j^*)^l = n(\varphi_i^*)^{n-1} (\varphi_j^*)^l \nabla(\varphi_i^*) + l(\varphi_i^*)^n (\varphi_j^*)^{l-1} \nabla(\varphi_j^*) \\ &= \begin{bmatrix} \nabla(\varphi_i^*) & \nabla(\varphi_j^*) \end{bmatrix} \begin{bmatrix} n(\varphi_i^*)^{n-1} (\varphi_j^*)^l \\ l(\varphi_i^*)^n (\varphi_j^*)^{l-1} \end{bmatrix}. \end{aligned}$$

For any $t \in I$ the vector $\begin{bmatrix} n(\varphi_i^*)^{n-1} (\varphi_j^*)^l & l(\varphi_i^*)^n (\varphi_j^*)^{l-1} \end{bmatrix}^T$ is constant. Therefore, the gradient of φ is in \mathcal{KG} .

Now we assume there exist k steps from the ancestors to φ . Let φ_1 and φ_2 be generated by $k-1$ steps. The induction assumption holds, meaning, their gradients are in \mathcal{KG} . Now, there is one step from φ_1 and φ_2 to φ . As shown, $\nabla\varphi$ is a linear combination of the gradients of its generators, $\nabla\varphi_1, \nabla\varphi_2$. But these vectors belong to \mathcal{KG} by the induction assumption. Therefore, $\nabla\varphi \in \mathcal{KG}$. ■

The multiplicity of Koopman eigenfunctions results from either arithmetical manipulations (Def. 3.11) or the existence of several time state-space mappings (Def. 3.3). The main difference is the rank of the Jacobian, $\mathcal{J}(\varphi)$. Given a vector of KEFs, adding another Koopman eigenfunction from the Koopman family of the KEF in the vector – does not increase the rank of the Jacobian. However, adding a Koopman eigenfunction from another time state-space mapping does. The Jacobian matrix rank is related to system controllability and observability (see for example [7, 20]). In the following, we formulate the connections between the rank of the Jacobian matrix, the size of the ancestor set, and time state-space mappings.

Definition 3.15 (Full observability in the context of Koopman theory). *Consider the dynamical system Eq. (2.1) where $\mathbf{x} \in \mathbb{R}^N$. The system is fully observable if the state-space can be revealed from the KEFs and the initial condition.*

Proposition 3.16 (Sufficient condition for full observability). *Consider the dynamical system (2.1) where $\mathbf{x} \in \mathbb{R}^N$. Let us denote the Koopman family of all Koopman eigenfunctions of the dynamics as \mathcal{K}_P . An ancestor set of \mathcal{K}_P is denoted as $\{\varphi_i^*\}_{i=1}^n$. The system is fully observable if $N \leq n$.*

Proof. According to Lemma 3.13, for any vector of KEFs the following equation holds,

$$(3.21) \quad \mathcal{J}(\varphi)P(\mathbf{x}) = \Lambda\varphi(\mathbf{x}), \quad (a.e.).$$

Let us choose a vector of ancestors, i.e.

$$(3.22) \quad \varphi^*(\mathbf{x}) = [\varphi_1^*(\mathbf{x}) \quad \cdots \quad \varphi_n^*(\mathbf{x})]^T.$$

According to Lemma 3.14 the rank of the Jacobian matrix is full and equal to N . Since the matrix $\mathcal{J}(\varphi)^T \mathcal{J}(\varphi)$ is invertible, the dynamics, P , can be revealed according to the following relation,

$$(3.23) \quad P(\mathbf{x}) = (\mathcal{J}(\varphi)^T \mathcal{J}(\varphi))^{-1} \mathcal{J}(\varphi)^T \Lambda\varphi(\mathbf{x}), \quad (a.e.).$$

The state-space can now be calculated as,

$$(3.24) \quad \mathbf{x}(t) = \mathbf{x}_0 + \int_a^t (\mathcal{J}(\boldsymbol{\varphi}(\tau))^T \mathcal{J}(\boldsymbol{\varphi}(\tau)))^{-1} \mathcal{J}(\boldsymbol{\varphi}(\tau))^T \Lambda \boldsymbol{\varphi}(\tau) d\tau. \quad \blacksquare$$

Corollary 3.17 (Sufficient condition for full observability). *If each entry in P is either positive or negative for any t in I then each entry of the state-space is monotone (and injective). We can formulate N different time state-space mappings from \mathcal{X} to I (Theorem 3.8). These mappings induce N different KEFs and according to Proposition 3.16 the system is fully observable.*

Remark 3.18 (Sufficient condition for dynamic reconstruction). If none of the entries of P is either positive or negative for all t in I then the dynamics can be reconstructed as

$$(3.25) \quad P(\mathbf{x}) = \mathcal{J}^{-1}(\boldsymbol{\varphi}) \Lambda \boldsymbol{\varphi}(\mathbf{x}).$$

According to Corollary 3.17, if none of the entry of P is zero in I then the Jacobian matrix is $N \times N$ and is full rank, therefore – inevitable. Using Th. 3.13 we reach Eq. (3.25).

Remark 3.19 (Global controllability). Reconstructing the dynamical system enables us to enlarge the *Region of Attraction* (ROA), Eq. (2.20). Given the nonlinear dynamics,

$$(3.26) \quad \frac{d}{dt} \mathbf{x}(t) = P(\mathbf{x}(t)) + \mathbf{u},$$

we can cancel the nonlinearity with the ancestors of a Koopman family $\boldsymbol{\varphi}(\mathbf{x})$ if the dynamics is fully observable. In order to reach a stable system for any point \mathbf{x} we define the following input \mathbf{u} ,

$$(3.27) \quad \mathbf{u} = \mathcal{J}^{-1}(\boldsymbol{\varphi}) \Lambda \boldsymbol{\varphi}(\mathbf{x}) + \mathbf{w},$$

where the first element cancels the nonlinearity of the system (Remark 3.18) and the second term brings the system to any desired point in \mathbb{R}^N . Note that we assume there are no singular points in P .

3.2.3. Koopman Mode Decomposition. The Koopman mode decomposition leverages this infinite family to reconstruct the observations from the Koopman eigenfunctions [39]. The reconstruction is a linear combination of Koopman eigenfunctions. For instance, the i th entry of \mathbf{x} is assumed to be reconstructed as [6],

$$(3.28) \quad x_i(t) = \sum_{j=1}^{\infty} v_{i,j} \varphi_j(\mathbf{x}(t)),$$

where $v_{i,j}$ is a scalar. Then, the state-space can be written as,

$$(3.29) \quad \mathbf{x}(t) = \sum_{j=1}^{\infty} \mathbf{v}_j \varphi_j(\mathbf{x}(t)),$$

where \mathbf{v}_j is an N dimensional vector whose entries are the coefficients of the j th Koopman eigenfunction, namely $\mathbf{v}_j = [v_{1,j} \ \cdots \ v_{N,j}]^T$. Substituting the solution of $\varphi(\mathbf{x})$, Eq. (KEF), we get,

$$(3.30) \quad \mathbf{x}(t) = \sum_{j=1}^{\infty} \mathbf{v}_j \varphi_j(\mathbf{x}(a)) e^{\lambda_j t}.$$

The infinite triplet $\{\mathbf{v}_j, \varphi_j, \lambda_j\}_{j=1}^{\infty}$ is the Koopman mode decomposition, where $\{\mathbf{v}_j\}_{j=1}^{\infty}$ are the Koopman modes, $\{\varphi_j\}_{j=1}^{\infty}$ are the KEFs, and $\{\lambda_j\}_{j=1}^{\infty}$ are the Koopman eigenvalues. Note that the maximal index argument in the sum of Eq. (3.29) is not necessarily infinity. For example, it is enough to have one mode to reconstruct the linear dynamics initiated with one of its eigenvectors. In matrix notations, let V be a matrix whose column vectors are the corresponding Koopman modes. The state-space can be expressed as,

$$(3.31) \quad \mathbf{x}(t) = V \boldsymbol{\varphi}(\mathbf{x}(t)).$$

Thus, the dynamical system has a linear representation with the measurements $\{\varphi_j(\mathbf{x})\}_{j=1}^{\infty}$ [26].

EXAMPLE 3.20 (KMD of Zero Homogeneous Dynamics). Let us consider the following dynamical system

$$(3.32) \quad \frac{d}{dt} \mathbf{x} = -P(\mathbf{x}), \quad \mathbf{x}(t=0) = \mathbf{v}, \quad I = [0, 1/\lambda)$$

where P is a zero homogeneous operator (admitting $P(a \cdot \mathbf{x}) = \text{sign}(a)P(\mathbf{x})$, $\forall a \in \mathbb{R}$), \mathbf{v} and λ are a nonlinear eigenvector and the corresponding eigenvalue of P , respectively, i.e. they admit the nonlinear eigenvalue problem $P(\mathbf{v}) = \lambda \mathbf{v}$. More background on such problems is presented in [24]. Then, the solution of the ODE is,

$$(3.33) \quad \mathbf{x}(t) = \mathbf{v}(1 - \lambda t), \quad t \in I.$$

A KEF can be formulated by the time state-space mapping as,

$$(3.34) \quad \varphi(t) = e^t = e^{\frac{1 - \langle \mathbf{x}, \mathbf{v} \rangle}{\|\mathbf{v}\|^2 \lambda}}.$$

We would like now to express the solution (3.33) with Koopman eigenfunctions. To express the function t we have to apply the natural logarithm, \ln , on the Koopman eigenfunction. With Taylor series one can express it as,

$$(3.35) \quad t = \ln(\varphi(\mathbf{x})) = \sum_{n=1}^{\infty} (-1)^{n+1} \frac{(\varphi(\mathbf{x}) - 1)^n}{n}.$$

Then, the solution in (3.33) can be written as,

$$(3.36) \quad \mathbf{x}(t) = \mathbf{v} \left(1 - \lambda \sum_{n=1}^{\infty} (-1)^{n+1} \frac{(\varphi(\mathbf{x}) - 1)^n}{n} \right).$$

By expanding the terms $(\varphi - 1)^n$ we get an infinite polynomial with respect to the KEF φ . KMD emerges naturally. ■

Discussion. According to this example, since there is only one mode and its decay profile is not exponential, there can be many KEFs for one Koopman mode. The multiplicity of eigenvalues for one mode is related to the limitations of DMD. Since DMD recovers only linear dynamics it cannot handle well one eigenvector with multiple eigenvalues.

We can now formulate the relation between Koopman modes and the dynamical system.

Proposition 3.21 (The Jacobian and Koopman modes). *Let $\varphi(\mathbf{x})$ be a vector of Koopman eigenfunctions and $\mathcal{J}(\varphi(\mathbf{x}))$ be its Jacobian matrix. In addition, let V be defined as in (3.31). Then, $P(\mathbf{x})$ is a right eigenvector of the matrix $V \cdot \mathcal{J}(\varphi(\mathbf{x}))$ with eigenvalue one.*

Proof. The time derivative of Eq. (3.31) is given by,

$$(3.37) \quad \begin{aligned} \frac{d}{dt} \mathbf{x} &= V \frac{d}{dt} \varphi(\mathbf{x}) \\ P(\mathbf{x}) &= V \mathcal{J}(\varphi(\mathbf{x})) P(\mathbf{x}). \end{aligned} \quad \blacksquare$$

EXAMPLE 3.22 (Nonlinear system). Given the following system,

$$(3.38) \quad \frac{d}{dt} \begin{bmatrix} x_1 \\ x_2 \end{bmatrix} = \begin{bmatrix} x_1 \\ x_2 - x_1^2 \end{bmatrix}, \quad \begin{bmatrix} x_1(0) \\ x_2(0) \end{bmatrix} = \begin{bmatrix} 1 \\ 1 \end{bmatrix}.$$

The solution is,

$$(3.39) \quad \begin{bmatrix} x_1 \\ x_2 \end{bmatrix} = \begin{bmatrix} 1 & 0 \\ 2 & -1 \end{bmatrix} \begin{bmatrix} e^t \\ e^{2t} \end{bmatrix}.$$

The time state-space mappings are,

$$(3.40) \quad \begin{aligned} t &= \ln(x_1), \\ t &= \frac{1}{2} \ln(2x_1 - x_2). \end{aligned}$$

By choosing $\alpha = 1$, $\beta = 0$, the Koopman eigenfunctions, following (3.5), are,

$$(3.41) \quad \begin{aligned} \varphi_1(\mathbf{x}) &= x_1, \\ \varphi_2(\mathbf{x}) &= \sqrt{2x_1 - x_2}. \end{aligned}$$

The state-space, $[x_1 \ x_2]^T$, can be reconstructed by these eigenfunctions as,

$$(3.42) \quad \begin{bmatrix} x_1 \\ x_2 \end{bmatrix} = \begin{bmatrix} \varphi_1(\mathbf{x}) \\ 2\varphi_1(\mathbf{x}) - \varphi_2(\mathbf{x})^2 \end{bmatrix} = \begin{bmatrix} 1 & 0 \\ 2 & -1 \end{bmatrix} \begin{bmatrix} \varphi_1(\mathbf{x}) \\ \varphi_2(\mathbf{x})^2 \end{bmatrix} = V \varphi(\mathbf{x}).$$

We observe there are two modes, $[1, 2]^T$ and $[0, -1]^T$, which evolve linearly under the nonlinear system (3.38). In addition, $V \mathcal{J}(\varphi(\mathbf{x})) = I_{2 \times 2}$, hence, $P(\mathbf{x})$ is an eigenvector for any \mathbf{x} . \blacksquare

We examined above the strong relation between the time state-space mapping and Koopman eigenfunctions. The following proposition states a limitation between the two notions.

Proposition 3.23 (Existence of Koopman eigenfunctions with no time state-space mapping). *The state-space mapping is not a necessary condition for the existence of Koopman eigenfunctions.*

Proof. This can be shown by the following simple example. Let us consider the linear system,

$$(3.43) \quad \frac{d}{dt} \mathbf{x} = A\mathbf{x}, \quad \mathbf{x}(t=0) = \mathbf{x}_0,$$

where A is an $N \times N$ matrix. For simplicity, we assume the eigenvalues, $\{\lambda_i\}_{i=1}^N$, are unique and the eigenvector set, $\{\mathbf{v}_i\}_{i=1}^N$, is orthonormal. Then, the solution of this system of equations can be written as,

$$(3.44) \quad \mathbf{x}(t) = \sum_{i=1}^N b_i \mathbf{v}_i e^{\lambda_i t},$$

where the vector $\mathbf{b} = [b_1 \ \dots \ b_N]^T$ is chosen according to the initial condition. To form the Koopman eigenfunctions and, correspondingly, the Koopman mode, one should formulate the time state-space mapping. For each eigenvector and eigenvalue of A there is a mapping, expressed as,

$$(3.45) \quad t_i(\mathbf{x}) = \frac{1}{\lambda_i} \ln \left(\frac{\mathbf{v}_i^T \mathbf{x}}{b_i} \right).$$

Thus, the Koopman eigenfunctions are,

$$(3.46) \quad \varphi_i(\mathbf{x}) = e^{t_i(\mathbf{x})} = \left(\frac{\mathbf{v}_i^T \mathbf{x}}{b_i} \right)^{\frac{1}{\lambda_i}}.$$

This expression can be simplified by applying Def. 3.11, yielding the following system,

$$(3.47) \quad \frac{d}{dt} \begin{bmatrix} \mathbf{v}_1^T \mathbf{x} \\ \vdots \\ \mathbf{v}_n^T \mathbf{x} \end{bmatrix} = \begin{bmatrix} \lambda_1 & & \\ & \ddots & \\ & & \lambda_n \end{bmatrix} \begin{bmatrix} \mathbf{v}_1^T \mathbf{x} \\ \vdots \\ \mathbf{v}_n^T \mathbf{x} \end{bmatrix}.$$

Note that if the eigenvector, \mathbf{v}_i , is complex then the time state-space mapping, Eq. (3.45), does not exist since it is not well defined. In this case, to create a time state-space mapping, we have to choose one branch from the \ln function. However, the Koopman eigenfunction, Eq. (3.46), has a unique value since the exponent cancels the ambiguity of the \ln function. It shows that a Koopman eigenfunction can exist in cases where the time state-space mapping does not. ■

4. Koopman Theory for PDE. Let us generalize these results to the continuous setting of the Koopman theory, following [40]. We consider the solution of Eq. (2.5), based on the following assumptions.

Assumption 4.1 (Proper Operator). *The operator $\mathcal{P}(f(x))$ in Eq. (2.5) is proper.*

Lemma 4.2 (Continuous u). *If the operator \mathcal{P} in Eq. (2.5) admits Assumption 4.1 then the solution is continuous in t .*

This is quite standard in the theory of PDEs. Basically, letting $u(x, t)$ to be the solution of Eq. (2.5), we can write a first order Taylor expansion for the variable t as,

$$(4.1) \quad u(x, t + dt) = u(x, t) + \mathcal{P}(u(x, t)) \cdot dt + o(dt).$$

Since the value of $\mathcal{P}(u(x, t))$ is finite, we get $|u(x, t + dt) - u(x, t)| \rightarrow 0$ as $dt \rightarrow 0$.

Assumption 4.3 (Fréchet Differentiability). *The operator \mathcal{P} is Fréchet differentiable a.e. in \mathcal{H} .*

If \mathcal{P} admits Assumption 4.3 then the solution $u(x, t)$ is in C^1 a.e. with respect to t (see e.g. [48]).

Definition 4.4 (Time mapping). *Let $u(x, t)$ be the solution of the dynamical system (2.5) where $t \in I$. Let $\Xi(u)$ (Ξ is capital ξ) be a functional mapping from the solution u to t , i.e.*

$$(4.2) \quad t = \Xi(u).$$

Lemma 4.5 (Differentiation of time mapping). *Let the Assumptions 4.1 and 4.3 hold. If the time mapping, $t = \Xi(u)$, exists then it admits the following,*

$$(4.3) \quad \langle \partial \Xi(u(x, t)), \mathcal{P}(u(x, t)) \rangle = 1 \quad \text{a.e. in } t \in I.$$

Proof. The mapping $\Xi(u(x))$ is in C^1 a.e. in $t \in I$ since $u(x, t) \in C^1$, a.e. with respect to t in I . The time derivative of the mapping is,

$$(4.4) \quad 1 = \frac{d}{dt} t = \frac{d}{dt} \Xi(u) = \langle \partial \Xi(u(x, t)), \frac{d}{dt} u(x, t) \rangle = \langle \partial \Xi(u(x, t)), \mathcal{P}(u(x, t)) \rangle.$$

And this expression is valid almost everywhere. ■

Proposition 4.6 (Condition for the inexistence of a Koopman eigenfunctional). *If there is an equilibrium point in I then a nontrivial Koopman eigenfunctional does not exist.*

Proof. Let $t_0 \in I$ be an equilibrium point and $\phi(u(x, t))$ be a Koopman eigenfunctional. Then, $u(x, t) = \text{const}$, $\forall t \in [t_0, b]$. Therefore, Eq. (2.8) does not hold for nontrivial ϕ for any $\lambda \neq 0$. ■

Remark on dynamics with finite time support. Remark 3.6 is valid also for dynamics of the form of Eq. (2.5). Namely, if there exists a time point, $T_{ext} \in I$, for which $\mathcal{P}(u(x, t)) = 0, \forall t > T_{ext}$, then there is no Koopman eigenfunctional for this dynamics.

Lemma 4.7 (Koopman eigenfunctionals induced by a time state-space mapping). *Let the Assumptions 4.1 and 4.3 hold and $u(x, t)$ be the solution of Eq. (2.5). If there exists a time mapping, $t = \Xi(u)$, then a Koopman eigenfunctional exists.*

Proof. Given the mapping, $t = \Xi(u)$, we define the following functional,

$$(4.5) \quad \phi(u) = e^{\alpha\Xi(u)+\beta}.$$

The time derivative of this functional is,

$$(4.6) \quad \begin{aligned} \frac{d}{dt}\phi(u(x,t)) &= \frac{d}{d\Xi}e^{\alpha\Xi(u(x,t))+\beta} \frac{d}{dt}\Xi(u(x,t)) = \alpha\phi(u(x,t))\langle\partial\Xi(u(x,t)), \frac{d}{dt}u(x,t)\rangle \\ &= \alpha\phi(u(x,t))\langle\partial\Xi(u(x,t)), \mathcal{P}(u(x,t))\rangle. \end{aligned}$$

According to Lemma 4.5, $\langle\partial\Xi(u(x,t)), \mathcal{P}(u(x,t))\rangle = 1$ a.e.. Thus, the function in Eq. (4.5) admits Eq. (KEFal) for any value of β , where the corresponding eigenvalue is $\lambda = \alpha$. ■

Theorem 4.8 (Sufficient condition for the existence of a Koopman eigenfunctional). *Let the Assumptions 4.1 and 4.3 hold, let $u(x,t)$ be the solution of Eq. (2.5), and let there be a real function $f : I \rightarrow L$, for which $u(f(t),t)$ is monotonic with respect to t . Then, Koopman eigenfunctionals exist in the time interval I .*

Proof. Let us define the following monotonic function,

$$(4.7) \quad g(t) = \int_0^L u(x,t)\delta(x-f(t))dx,$$

where δ is the Dirac delta. Then, the time mapping is

$$(4.8) \quad t = \Xi(u) = g^{-1}\left(\int_0^L u(x,t)\delta(x-f(t))dx\right).$$

According to Lemma 4.7 there exists a eigenfunctional, which can be expressed by Eq. (4.5). ■

5. Mode Decomposition based on Time State-Space Mapping. DMD can be viewed as an exponential data fitting algorithm [31]. As such, it is an implementation of KMD when the KEFs are in the form of Eq. (3.46). The limitations of DMD are apparent when the typical decay profile of the dynamics is not exponential. For example, the typical decay profile for homogeneous flows is polynomial (with finite extinction time) [16]. This problem was analyzed and addressed in [13]. Another implicit assumption of DMD is that the modes are valid for the entire interval I . For example, the gradient descent flow with respect to the total variation energy cannot be reconstructed by DMD [14]. Here, we suggest a new approach for mode decomposition based on time decay profiles typical to the dynamics.

Monotone time function dictionaries. In recent years, machine learning methods were employed in the design of advanced DMD algorithms, such as *Extended DMD* (EDMD) [49, 50, 51] and *kernel DMD* (KDMD) [28]. Several learning-based approaches suggested to build a data-driven dictionary to reconstruct the dynamics sparsely [3, 33, 42, 44]. These works focus on learning the spatial structures that approximate Koopman modes. In other words, these algorithms aim at finding measurements that evolve linearly under the dynamical system.

This direction has some limitations, most notably for decaying processes, since the reconstruction of KEFs may be infinite-dimensional. The reconstruction of a KEF as a polynomial

of the observation, as in Example 3.9, contains an infinite vector of measurements. On the other hand, our approach is based on the assumption that the observed dynamic has a typical monotone decay profile within a given time interval. Thus, instead of focusing on measurements that decay exponentially, the focus of our algorithm is on finding spatial structures that decay according to a predefined family of profiles.

Koopman Modes. Let us assume the dynamics induces a known typical monotone profile for different spatial structures in the data. The profile, denoted as $a_{\lambda_i}(t)$, varies according to the spatial structure and depends on a parameter λ_i . Given the time sampling point set $\{t_i\}_0^M$ (not to be confused with time state-space mapping), we define the overcomplete dictionary,

$$(5.1) \quad \mathcal{D} = \begin{bmatrix} a_{\lambda_0} t_0 & \cdots & a_{\lambda_0} t_M \\ & \vdots & \\ a_{\lambda_L} t_0 & \cdots & a_{\lambda_L} t_M \end{bmatrix},$$

where L is large enough. An atom of this dictionary is a row. Since the time function $a_{\lambda_i}(t)$ is monotone there exists an inverse function for each atom, denoted as,

$$(5.2) \quad t = \xi(a_{\lambda_i}(t)).$$

In matrix formulation, for a discrete time setting, this can be written as,

$$(5.3) \quad \mathbf{t} = \boldsymbol{\xi}(\mathcal{D}),$$

where $\mathbf{t} \in \mathbb{R}^{(L+1) \times M}$. It is assumed that there exists a (sparse) mode matrix V which can approximate the samples of the system X using the dictionary by,

$$(5.4) \quad X = V\mathcal{D} + e,$$

where $X = [\mathbf{x}_0 \cdots \mathbf{x}_M]$ and e is a small error term.

Dimensionality Reduction. Following the assumption of DMD, we would like to obtain a sparse representation of modes. This problem has been thoroughly investigated and can be formulated as [35],

$$(5.5) \quad \min_V \|X - V\mathcal{D}\|_F^2, \quad s.t. \|V\|_0 \leq r,$$

where $\|V\|_0 < r$ indicates the requirement that only up to r columns in V are not zero. This problem is NP-hard and the sparsity constraint is relaxed to solving the following minimization problem,

$$(5.6) \quad \min_V \|X - V\mathcal{D}\|_F^2 + \lambda \|V\|_1.$$

The solution of (5.6) is the minimizer of the left term when the nonzero entries in each mode are at least λ (see algorithm 6 p. 153 in [35]).

In general, there are several well known algorithms to recover the modes when the dictionary is known (see [19]). We note that our problem is somewhat more difficult than the common signal processing case since the atoms in the dictionary are highly coherent (strongly

correlated). Here, we apply the implementation from [36] for the Lasso algorithm (Eq. (5.6)) with a fine-tuning post-processing stage (Appendix B) to solve this problem. The output of this algorithm is \hat{V} and $\hat{\mathcal{D}}$, where each column in the matrix \hat{V} contains a mode and $\hat{\mathcal{D}}$ has the corresponding atoms, taken from the dictionary \mathcal{D} . The entire dynamics can be approximated as,

$$(5.7) \quad X \approx \hat{V}\hat{\mathcal{D}},$$

where \approx denotes equality in the sense of Eq. (5.6).

Approximation of Koopman eigenfunctions. Given the modes \hat{V} and the data matrix X and assuming $\hat{V}^T\hat{V}$ is invertible, one can express the dictionary as

$$(5.8) \quad \hat{\mathcal{D}} \approx (\hat{V}^T\hat{V})^{-1}\hat{V}^T X.$$

This reconstruction of the dictionary is necessary to be in the argument of the time state-space mapping, Eqs. (5.2) and (5.3), as follows,

$$(5.9) \quad \mathbf{t} = \boldsymbol{\xi}(\hat{\mathcal{D}}) = \boldsymbol{\xi}((\hat{V}^T\hat{V})^{-1}\hat{V}^T X).$$

Thus, we can express with the dynamic measurements an exponential function. According to Eq. (3.5), the KEFs are given by,

$$(5.10) \quad \varphi(X) = e^{\mathbf{t}(X)} = e^{\boldsymbol{\xi}((\hat{V}^T\hat{V})^{-1}\hat{V}^T X)}.$$

We summarize this algorithm in Algo. 5.1.

Algorithm 5.1 Koopman Mode Approximation

1: **Inputs:**

 Data sequence $\{\mathbf{x}_k\}_0^N$ and typical profile $a_\lambda(t)$.

2: Find modes \hat{V} and dictionary $\hat{\mathcal{D}}$ (for example invoke Algo B.1).

3: Formulate the decay profiles with the modes \hat{V} and the data X , Eq. (5.8).

4: Formulate the time state-space mapping, Eq. (5.9).

5: **Outputs:**

 Extract KEFs from the observations by Eq. (5.10).

Approximation of KMD. *Koopman Mode Decomposition* can be expressed by Koopman modes V and KEFs using the time variable t and its powers. In the same way, the typical decay profile $a_{\lambda_i}(t)$ can be expressed using a Taylor series (under sufficient smoothness conditions). Then, by variation of parameter, the KMD is obtained (see Example 3.20).

Note that the above presentation is only intended to show a possible algorithmic path that is implied by our analysis. We limit the scope of our discussion here and leave for future work important issues, such as spectrum and system reconstruction accuracy, dimensionality reduction, robustness to noise, and prediction capacity [21, 34].

6. Examples. In this section, we apply the theory to a few examples. We examine the following: system reconstruction; global controllability; mode decomposition based on a dictionary of monotone profiles; and finding eigenfunctionals in partial differential equations.

EXAMPLE 6.1 (System Reconstruction and Global Controllability). This example is based on [38] (p. 10). Given the system,

$$(6.1) \quad \frac{d}{dt}x(t) = P(x) + u = x - x^3 + u,$$

we would like to obtain global controllability via a Koopman eigenfunction according to Remark 3.19. Note that there are three equilibrium points $-1, 0$ and 1 with ROAs: $\mathcal{RA}(-1) = (-\infty, 0)$, $\mathcal{RA}(0) = \{0\}$, and $\mathcal{RA}(1) = (0, \infty)$, respectively. The solution of this equation is,

$$(6.2) \quad t(x) = \ln\left(\frac{x}{\sqrt{1-x^2}}\right) + C.$$

According to Theorem 3.8 one of the Koopman eigenfunctions is,

$$(6.3) \quad \varphi(x) = e^{t(x)} = \frac{x}{\sqrt{1-x^2}}.$$

We set the input u to,

$$(6.4) \quad u = -\mathcal{J}(\varphi)^{-1}\varphi + w,$$

where w is the input after feedback linearization. The Jacobian matrix is simply the derivative of φ with respect to x ,

$$(6.5) \quad \mathcal{J}(\varphi) = (1-x^2)^{-\frac{3}{2}},$$

yielding,

$$(6.6) \quad u = -\mathcal{J}(\varphi)^{-1}\varphi + w = -(1-x^2)^{\frac{3}{2}}\frac{x}{\sqrt{1-x^2}} + w = -x(1-x)^2 + w.$$

Substituting this input in the dynamical system, Eq. (6.1), we get the following,

$$(6.7) \quad \frac{d}{dt}x(t) = P(x) + u = x - x^3 + u = x - x^3 - x(1-x)^2 + w = w.$$

This system is linear and controllable. The system can get any value in the state space, for example, we can set $w = -(x - x^*)$, where x^* is the desired equilibrium point. ■

EXAMPLE 6.2 (Total Variation eigenfunctional). Very common PDE in image processing is the gradient descent flow with respect to the total-variation (TV) functional [2, 8, 11, 23, 43], which for smooth functions u can be expressed as,

$$(6.8) \quad J_{TV}(u(x)) = \langle |\nabla u(x)|, 1 \rangle.$$

The gradient descent flow for this non-smooth convex functional is defined by,

$$(6.9) \quad u_t = \mathcal{P} \in -\partial J_{TV}(u), \quad u(t=0) = u_0,$$

where $\partial J_{TV}(u)$ denotes the subdifferential of TV at u . The flow is known also as the 1-Laplacian flow. When $x \in \mathbb{R}$ the solution is piece-wise linear, at any time interval \mathcal{I}_j the solution admits, [14]

$$(6.10) \quad u(x, t) = h_{1,j}(x) + h_{2,j}\lambda_j t.$$

In addition, it was shown [10, 14] that the two modes are orthogonal, $h_{1,j} \perp h_{2,j}$. Thus, at each interval there are two eigenfunctionals, the trivial one and the second one, corresponding to the linearly evolving mode,

$$(6.11) \quad \phi(u) = e^{\frac{\langle h_{2,j}, u \rangle}{\|h_{2,j}\|^2 \lambda_j}}. \quad \blacksquare$$

EXAMPLE 6.3 (Nonlinear PDE # 2). Let the solution of Eq. (2.5) be,

$$(6.12) \quad u(x, t) = v_1(x) \cdot a_1(t) + v_2(x) \cdot a_2(t).$$

The solution $u(x, t)$ and the spatial structures $v_i(x)$, $i \in \{1, 2\}$, are depicted in Fig. 1. The decay profile is of the form of $a_i(t) = (1 + \lambda_i t)^+$, where $\lambda_1 = 1/10$ and $\lambda_2 = 1/30$. DMD yields

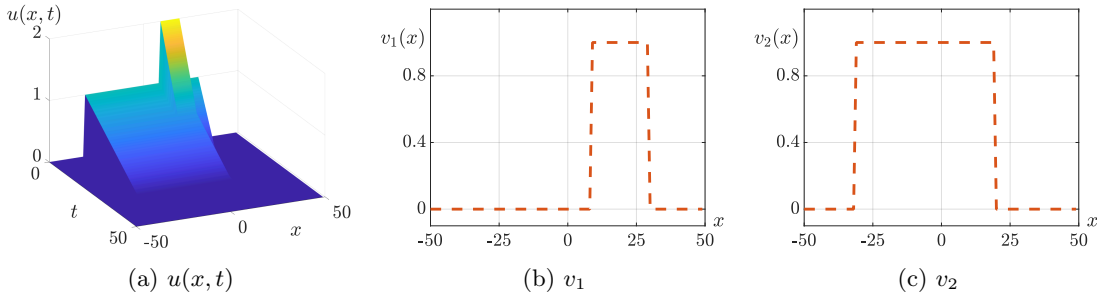


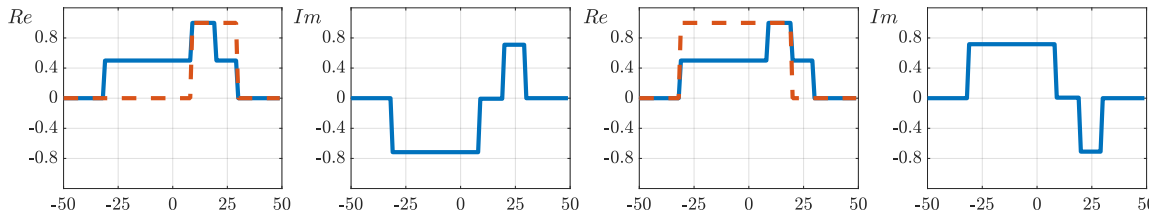
Figure 1. (a) The solution of Eq. (6.12). On the right, the spatial structures (modes), v_1 (b) and v_2 (c). They evolve with linear decay at a rate of $\lambda_1 = 1/10$ and $\lambda_2 = 1/30$, respectively.

the decomposition depicted in Fig. 2. The modes are complex and each of them is depicted in two graphs, the real and the imaginary parts (Fig. 2a). It demonstrates the limitations of DMD in systems with typical dynamics which are not exponential.

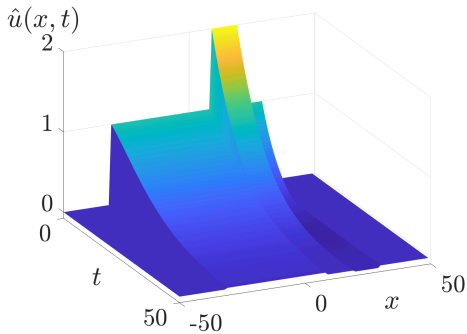
The decomposition resulted from Algo. B.1 is depicted in Fig. 3. The modes are shown in Fig. 3a and recover the modes accurately. The entire dynamics reconstruction is given in Fig 3b with the corresponding error in Fig. 3c. Having the modes, we can find the eigenfunctionals,

$$(6.13) \quad \phi(t) = \begin{bmatrix} \langle v_1, v_1 \rangle & \langle v_1, v_2 \rangle \\ \langle v_2, v_1 \rangle & \langle v_2, v_2 \rangle \end{bmatrix}^{-1} \begin{bmatrix} \langle v_1(x), u(x, t) \rangle \\ \langle v_2(x), u(x, t) \rangle \end{bmatrix} - \begin{bmatrix} 1 \\ 1 \end{bmatrix}. \quad \blacksquare$$

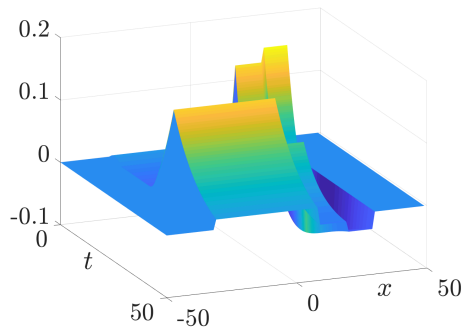
They are depicted in Fig. 4. One can see that the eigenfunctionals are valid until the vanishing points. The first mode vanishes at $t = 10$ and the second at $t = 30$.



(a) **Dynamic Mode Decomposition.** Two plots on the left: real and imaginary values of the first DMD mode, compared to v_1 (dashed). Two plots on the right: real and imaginary values of the second DMD mode, compared to v_2 (dashed).



(b) **Reconstruction**



(c) **Error $u(x, t) - \hat{u}(x, t)$**

Figure 2. Dynamic Mode Decomposition and Reconstruction. Top row: First two DMD modes, compared to v_i . Bottom row: Reconstruction through Eq. (2.9) (left) and the corresponding error (right). We can observe the dynamics is not reconstructed well and the error is significant.

7. Conclusion. This work discusses necessary and sufficient conditions for the existence of Koopman eigenfunctions. We examine KMD, system reconstruction, global linearity, controllability, and observability through Koopman theory. These insights highlight some limitations of DMD.

Dynamic Mode Decomposition accurately evaluates KMD as long as KEFs are linear combinations of the observations and KMD is finite-dimensional. However, DMD has clear limitations in four different settings: 1) The typical decay profile of the system is not exponential; 2) One Koopman mode is associated with multiple eigenvalues; 3) There is an equilibrium point in the time interval I ; 4) Koopman modes do not exist for all t in I . Another limitation emerges when the dynamic P is in C^0 almost everywhere. In this case, some of the modes might vanish at different times, as we see in the total-variation flow.

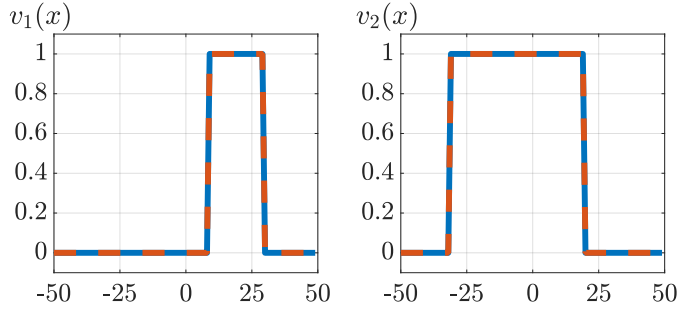
We suggest a new type of decomposition to overcome these fundamental problems. It is based on inverse time state-space mapping of injective curves. We implement this method using overcomplete dictionaries of monotone profiles, typical to the dynamics. This decomposition coincides with a basic assumption of DMD – the data can be sparsely represented.

List of Symbols

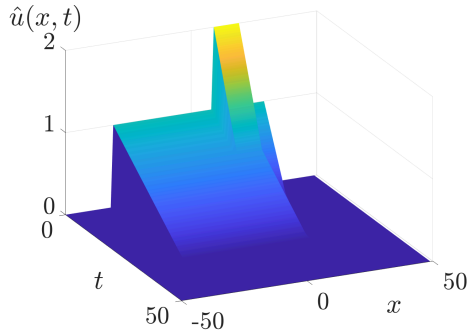
\mathbf{x}_i The i the sample of the state vector belongs to \mathbb{R}^N

X	Contains the samples of the dynamics $X = [\mathbf{x}_0 \cdots \mathbf{x}_M]$ belongs to $\mathbb{R}^{N \times (M+1)}$
\mathcal{U}	A matrix where $\mathcal{U}_{i,j} = u(x_i, t_j)$
H	A auto-correlation matrix of the set $\{h_i\}_{i=1}^M$
$\mathbf{H}\mathbf{u}$	A vector where $\mathbf{H}\mathbf{u}_i = \langle h_i(x), u(x, t) \rangle$
$\mathbf{h}(x)$	A vector $\mathbf{h}_i(x) = h_i(x)$
\mathcal{V}	Contains the main spatial structures $\{\mathbf{v}_i\}$
\mathcal{D}	A dictionary of a family of a decay profile
P	A (nonlinear) function $P : \mathbb{R}^N \rightarrow \mathbb{R}^N$ in C^1 a.e.
t	Time index where $t \in \mathbb{R}^+$
g	This is an observation function of the state vector \mathbf{x} , $g : \mathbb{R}^N \rightarrow \mathbb{R}$
K_P^T	The Koopman operator. The superscript denotes the time parameter and the subscript denotes the dynamical system
I	An interval $[a, b]$ in the time axis
$\varphi(\mathbf{x}(t))$	A Koopman eigenfunction
λ	A Koopman eigenvalue
∇	The gradient of a function
T	denotes the transform
\mathcal{H}	A Hilbert space
\mathcal{P}	An (nonlinear) operator $\mathcal{P} : \mathcal{H} \rightarrow \mathcal{H}$
Q	A (nonlinear) proper, lower-semicontinuous functional $Q : \mathcal{H} \rightarrow \mathbb{R}$
$\phi(\cdot)$	A Koopman eigenfunctional
\mathbf{v}_i	A preserved spatial shape under the dynamics P
$h_i(x)$	A preserved spatial shape under the dynamics \mathcal{P}
$a_i(t)$	The time function corresponding to the i th preserved spatial shape
$\gamma, \gamma - 1$	Denote the homogeneity degrees of a functional and its variational derivative, respectively.
X_0^{M-1}, X_1^M	Data matrices $[\mathbf{x}_0, \cdots, \mathbf{x}_{M-1}], [\mathbf{x}_1, \cdots, \mathbf{x}_M]$
U, Σ, V	<i>Singular Value Decomposition</i> (SVD) of \mathbf{x}_0^{N-1}
U_r, V_r	Sub-matrices of U, V containing the first r columns
Σ_r	Sub-matrix of Σ containing the most significant r eigenvalues of the SVD which are the diagonal of Σ
\mathcal{X}	The curve in \mathbb{R}^N representing the solution \mathbf{x}
$\xi(\cdot)$	A mapping from the curve $\mathbf{x}(t)$ to the time variable t
$\varphi(\mathbf{x})$	A Koopman mode
$\mathcal{J}(\varphi(\mathbf{x}))$	The Jacobian of Koopman mode $\varphi(\mathbf{x})$
Ξ	A functional mapping from $u(x, t)$ to t
ϕ	An eigenfunctional

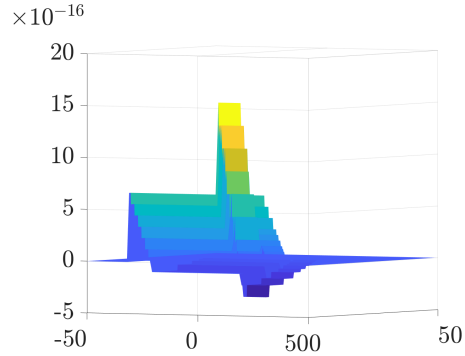
Appendix A. The Dynamic Mode Decomposition steps.



(a) **Sparse Mode Decomposition** - The modes resulting from Algo. B.1 (blue) and the actual modes of the dynamics (dashed red).

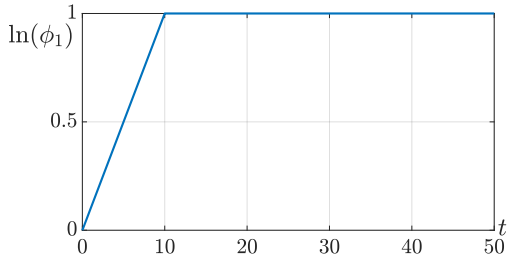


(b) **Reconstruction**

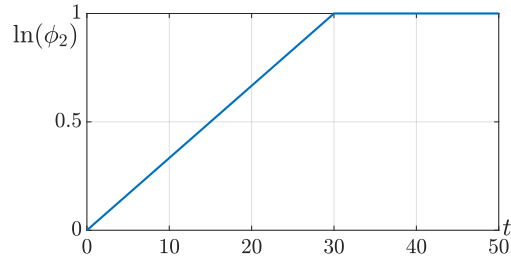


(c) **Error** $u(x, t) - \hat{u}(x, t)$

Figure 3. Sparse Mode Decomposition and Reconstruction (Algo. B.1) - (a) Sparse mode decomposition compared to the modes, v_1 and v_2 . (b) Dynamic reconstruction with Algo. B.1 (Eq. (5.7)) (c) The corresponding error. Correct modes are obtained yielding close to perfect reconstruction of the dynamics.



(a) Eigenfunctional #1



(b) Eigenfunctional #2

Figure 4. Eigenfunctionals - based on the monotone decay profile dictionary. These are the eigenfunctionals formulated in Eq. (6.13).

Coordinate representation. Given N observations of the dynamical system, Eq. (2.1), we form the data matrices as

$$(A.1) \quad X_0^{M-1} = [\mathbf{x}_0, \mathbf{x}_1, \dots, \mathbf{x}_{M-1}], \quad X_1^M = [\mathbf{x}_1, \mathbf{x}_2, \dots, \mathbf{x}_M] \in \mathbb{R}^{N \times M}$$

where $\mathbf{x}_k = \mathbf{x}(t_k)$. To find the spatial structures the SVD is applied on the data matrix,

$$(A.2) \quad X_0^{M-1} = U\Sigma V^*.$$

where V^* is the conjugate transpose of V . The columns of U span the column space of X_0^{M-1} . Thus, the spatial structures are represented by its coordinates

$$(A.3) \quad \mathbf{c}_k = U^* \mathbf{x}_k.$$

Dimensionality reduction. Assuming the data is embedded in subspace spanned by the first r columns of U . Then, the coordinates related to that subspace is

$$(A.4) \quad \mathbf{c}_{r,k} = U_r^* \cdot \mathbf{x}_k.$$

Linear mapping. Following the second assumption of the DMD, there is a linear mapping, F , from $\mathbf{c}_{r,k}$ to $\mathbf{c}_{r,k+1}$. The linear mapping, F , minimizes the DMD error, given by

$$(A.5) \quad F = \arg \min_F \left\| F \cdot C_{r,0}^{M-1} - C_{r,1}^M \right\|_{\mathcal{F}}^2,$$

where $\|\cdot\|_{\mathcal{F}}$ denotes the Frobenius norm and

$$(A.6) \quad C_{r,0}^{M-1} = U_r^* X_0^{M-1}, \quad C_{r,1}^M = U_r^* X_1^M.$$

The linear mapping, F , is the optimal linear mapping in the sense of the DMD error, Eq. (A.4), and we write the coordinate dynamic as

$$(A.7) \quad \mathbf{c}_{r,k+1} \approx F \cdot \mathbf{c}_{r,k}.$$

Then, we can write the dynamic for all k as

$$(A.8) \quad \mathbf{c}_{r,k} \approx F^k \cdot \mathbf{c}_{r,0}.$$

Modes, eigenvalues, and coefficients. Now, we would like to summarize the discussion above and to depict the dynamics as a linear system. In general, we can reconstruct a sample at step k from its coordinates as

$$(A.9) \quad \tilde{\mathbf{x}}_k = U_r \mathbf{c}_{r,k}.$$

In addition, if F is diagonalizable it can be formulated as

$$(A.10) \quad F = WDW^{-1},$$

where W contains the right eigenvectors of F , and D is a diagonal matrix whose entries are the eigenvalues of F .

Then, the dynamic can be simplified as

$$(A.11) \quad \tilde{\mathbf{x}}_k \approx U_r \cdot F^k \cdot U_r^* \mathbf{x}_0 = U_r \cdot W D^k W^{-1} \cdot U_r^* \mathbf{x}_0$$

Now, let us define the modes, $\{\phi_i\}_{i=1}^r$, eigenvalues, $\{\mu_i\}_{i=1}^r$, and coefficients, $\{\alpha_i\}_{i=1}^r$.

Modes are defined as $\Phi = [\phi_1 \ \cdots \ \phi_r] = U_r W$.

Eigenvalues are the diagonal entries of the matrix D , $\{\mu_i\}_{i=1}^r$.

Coefficients are defined by $\alpha = [\alpha_1 \ \cdots \ \alpha_r]^T = W^{-1} U_r^* \mathbf{x}_0$.

We can now reconstruct the approximate dynamics as,

$$(A.12) \quad \tilde{\mathbf{x}}_k \approx \Phi D^k \alpha = \sum_{i=1}^r \alpha_i \mu_i^k \phi_i.$$

Appendix B. Sparse Representation. The main focus should be put on the time function of the dynamic since the Koopman theory is based on that. In addition, we assume the dynamics induces a family of monotonic time functions, \mathcal{D} , where they differ by their parameters. For example, in linear systems, these functions are exponential, in zero-homogeneous dynamical systems the functions are linear with different slopes.

We assume the typical decay profile is known and we find the nonzero mode for example with the Lasso algorithm [35]. Then, we remove the not relevant modes and the corresponding atoms in the dictionary. We elaborate the algorithm in Algo. B.1

Acknowledgements. We would like to thank Prof. Gershon Wolansky from Department of Mathematics, Technion and Dr. Eli Appelboim from Electrical and Computer Engineering Department for stimulating discussions.

REFERENCES

- [1] T. ASKHAM AND J. N. KUTZ, *Variable projection methods for an optimized dynamic mode decomposition*, SIAM Journal on Applied Dynamical Systems, 17 (2018), pp. 380–416.
- [2] G. BELLETTINI, V. CASELLES, AND M. NOVAGA, *The total variation flow in rn* , Journal of Differential Equations, 184 (2002), pp. 475–525.
- [3] E. M. BOLLT, *Geometric considerations of a good dictionary for koopman analysis of dynamical systems: Cardinality, “primary eigenfunction,” and efficient representation*, Communications in Nonlinear Science and Numerical Simulation, (2021), p. 105833.
- [4] H. BREZIS, *Opérateurs maximaux monotones et semi-groupes de contractions dans les espaces de Hilbert*, Elsevier, 1973, p. 73.
- [5] S. L. BRUNTON, B. W. BRUNTON, J. L. PROCTOR, AND J. N. KUTZ, *Koopman invariant subspaces and finite linear representations of nonlinear dynamical systems for control*, PloS one, 11 (2016), p. e0150171.
- [6] S. L. BRUNTON, M. BUDIŠIĆ, E. KAISER, AND J. N. KUTZ, *Modern koopman theory for dynamical systems*, arXiv preprint arXiv:2102.12086, (2021).
- [7] S. L. BRUNTON AND J. N. KUTZ, *Data-driven science and engineering: Machine learning, dynamical systems, and control*, Cambridge University Press, 2019, pp. 276–320.
- [8] L. BUNGERT, M. BURGER, A. CHAMBOLLE, AND M. NOVAGA, *Nonlinear spectral decompositions by gradient flows of one-homogeneous functionals*, arXiv preprint arXiv:1901.06979, (2019).
- [9] L. BUNGERT, M. BURGER, AND D. TENBRINCK, *Computing nonlinear eigenfunctions via gradient flow extinction*, in International Conference on Scale Space and Variational Methods in Computer Vision, Springer, 2019, pp. 291–302.
- [10] M. BURGER, G. GILBOA, M. MOELLER, L. ECKARDT, AND D. CREMERS, *Spectral decompositions using one-homogeneous functionals*, SIAM Journal on Imaging Sciences, 9 (2016), pp. 1374–1408.
- [11] M. BURGER AND S. OSHER, *A guide to the tv zoo*, in Level set and PDE based reconstruction methods in imaging, Springer, 2013, pp. 1–70.

Algorithm B.1 Sparse Representation

- 1: **Inputs:**
Data sequence $\{\mathbf{x}_k\}_0^M$ and decay dictionary \mathcal{D}
- 2: **Initialize:**
 $\mathcal{SR} = \emptyset$
- 3: Find the sparse representation V according to [36].
- 4: Let \mathcal{I} be the set of indices of the atoms in \mathcal{D} sorted (from low to high) according to the norm of the modes (column vectors of V).
- 5: Remove from \mathcal{I} the indices for which the modes are zeros.
- 6: **while** True **do**
- 7: Define $\hat{\mathcal{D}}$ as a new dictionary containing the atoms with indices \mathcal{I} .
- 8: Compute $\hat{V} = X\hat{\mathcal{D}}^T(\hat{\mathcal{D}}\hat{\mathcal{D}}^T)^{-1}$
- 9: Compute the error $\|X - \hat{V}\hat{\mathcal{D}}\|_F^2$
- 10: Add the set \mathcal{I} and its corresponding error to \mathcal{SR}
- 11: Remove the first index in \mathcal{I} .
- 12: **if** \mathcal{I} is empty **then**
- 13: Break
- 14: **end if**
- 15: **end while**
- 16: Find in \mathcal{SR} the set of indices \mathcal{I} that yields the minimum error
- 17: Define $\hat{\mathcal{D}}$ as a new dictionary containing the atoms with indices \mathcal{I} .
- 18: Compute $\hat{V} = X\hat{\mathcal{D}}^T(\hat{\mathcal{D}}\hat{\mathcal{D}}^T)^{-1}$
- 19: **Outputs:**

$$\hat{V}, \hat{\mathcal{D}}$$

- [12] M. CHUAQUI, *General criteria for curves to be simple*, Journal of Mathematical Analysis and Applications, 464 (2018), pp. 955–963.
- [13] I. COHEN, O. AZENCOT, P. LIFSHITS, AND G. GILBOA, *Modes of homogeneous gradient flows*, arXiv preprint arXiv:2007.01534, (2020).
- [14] I. COHEN, T. BERKOV, AND G. GILBOA, *Total-variation mode decomposition*, in Scale Space and Variational Methods in Computer Vision, A. Elmoataz, J. Fadili, Y. Quéau, J. Rabin, and L. Simon, eds., Cham, 2021, Springer International Publishing, pp. 52–64.
- [15] I. COHEN AND G. GILBOA, *Shape Preserving Flows and the p -Laplacian Spectra*. working paper or preprint, Oct. 2018, <https://hal.archives-ouvertes.fr/hal-01870019>.
- [16] I. COHEN AND G. GILBOA, *Introducing the p -laplacian spectra*, Signal Processing, 167 (2020), p. 107281.
- [17] R. COURANT AND F. JOHN, *Introduction to calculus and analysis I*, Springer Science & Business Media, 2012.
- [18] S. T. DAWSON, M. S. HEMATI, M. O. WILLIAMS, AND C. W. ROWLEY, *Characterizing and correcting for the effect of sensor noise in the dynamic mode decomposition*, Experiments in Fluids, 57 (2016), p. 42.
- [19] M. ELAD, *Sparse and redundant representations: from theory to applications in signal and image processing*, Springer Science & Business Media, 2010.
- [20] E. EVANGELISTI, *Controllability and Observability: Lectures given at a Summer School of the Centro Internazionale Matematico Estivo (CIME) held in Pontecchio (Bologna), Italy, July 1-9, 1968*, vol. 46,

- Springer Science & Business Media, 2011.
- [21] M. GAVISH AND D. L. DONOHO, *The optimal hard threshold for singular values is $4/\sqrt{3}$* , IEEE Transactions on Information Theory, 60 (2014), pp. 5040–5053.
 - [22] G. GILBOA, *A spectral approach to total variation*, in International Conference on Scale Space and Variational Methods in Computer Vision, Springer, 2013, pp. 36–47.
 - [23] G. GILBOA, *A total variation spectral framework for scale and texture analysis*, SIAM journal on Imaging Sciences, 7 (2014), pp. 1937–1961.
 - [24] G. GILBOA, *Nonlinear Eigenproblems in Image Processing and Computer Vision*, Springer, 2018, pp. 133–140.
 - [25] M. S. HEMATI, C. W. ROWLEY, E. A. DEEM, AND L. N. CATTAFESTA, *De-biasing the dynamic mode decomposition for applied koopman spectral analysis of noisy datasets*, Theoretical and Computational Fluid Dynamics, 31 (2017), pp. 349–368.
 - [26] E. KAISER, J. N. KUTZ, AND S. BRUNTON, *Data-driven discovery of koopman eigenfunctions for control*, Machine Learning: Science and Technology, (2021).
 - [27] O. KATZIR, *On the scale-space of filters and their applications*, master’s thesis, Technion — Israel Institute of Technology, Haifa 3200003, March 2017.
 - [28] Y. KAWAHARA, *Dynamic mode decomposition with reproducing kernels for koopman spectral analysis*, Advances in neural information processing systems, 29 (2016), pp. 911–919.
 - [29] B. O. KOOPMAN, *Hamiltonian systems and transformation in hilbert space*, Proceedings of the national academy of sciences of the united states of america, 17 (1931), p. 315.
 - [30] M. KORDA AND I. MEZIĆ, *Linear predictors for nonlinear dynamical systems: Koopman operator meets model predictive control*, Automatica, 93 (2018), pp. 149–160.
 - [31] J. N. KUTZ, S. L. BRUNTON, B. W. BRUNTON, AND J. L. PROCTOR, *Dynamic mode decomposition: data-driven modeling of complex systems*, SIAM, 2016.
 - [32] J. N. KUTZ, J. L. PROCTOR, AND S. L. BRUNTON, *Koopman theory for partial differential equations*, arXiv preprint arXiv:1607.07076, (2016).
 - [33] Q. LI, F. DIETRICH, E. M. BOLLT, AND I. G. KEVREKIDIS, *Extended dynamic mode decomposition with dictionary learning: A data-driven adaptive spectral decomposition of the koopman operator*, Chaos: An Interdisciplinary Journal of Nonlinear Science, 27 (2017), p. 103111.
 - [34] H. LU AND D. M. TARTAKOVSKY, *Prediction accuracy of dynamic mode decomposition*, SIAM Journal on Scientific Computing, 42 (2020), pp. A1639–A1662.
 - [35] J. MAIRAL, F. BACH, J. PONCE, ET AL., *Sparse modeling for image and vision processing*, Foundations and Trends® in Computer Graphics and Vision, 8 (2014), pp. 85–283.
 - [36] J. MAIRAL, F. BACH, J. PONCE, G. SAPIRO, R. JENATTON, AND G. OBOZINSKI, *Spams: A sparse modeling software, v2. 6*, URL <http://spams-devel.gforge.inria.fr/downloads.html>, (2014).
 - [37] A. MAUROY, *Koopman operator theory for infinite-dimensional systems: Extended dynamic mode decomposition and identification of nonlinear pdes*, arXiv preprint arXiv:2103.12458, (2021).
 - [38] A. MAUROY, Y. SUSUKI, AND I. MEZIĆ, *The Koopman Operator in Systems and Control*, Springer, 2020.
 - [39] I. MEZIĆ, *Spectral properties of dynamical systems, model reduction and decompositions*, Nonlinear Dynamics, 41 (2005), pp. 309–325.
 - [40] H. NAKAO AND I. MEZIĆ, *Spectral analysis of the koopman operator for partial differential equations*, Chaos: An Interdisciplinary Journal of Nonlinear Science, 30 (2020), p. 113131.
 - [41] S. E. OTTO AND C. W. ROWLEY, *Koopman operators for estimation and control of dynamical systems*, Annual Review of Control, Robotics, and Autonomous Systems, 4 (2021).
 - [42] S. PAN, N. ARNOLD-MEDABALIMI, AND K. DURAISAMY, *Sparsity-promoting algorithms for the discovery of informative koopman-invariant subspaces*, Journal of Fluid Mechanics, 917 (2021).
 - [43] L. I. RUDIN AND S. OSHER, *Total variation based image restoration with free local constraints*, in Image Processing, 1994. Proceedings. ICIP-94., IEEE International Conference, vol. 1, IEEE, 1994, pp. 31–35, <https://doi.org/10.1109/ICIP.1994.413269>.
 - [44] S. H. RUDY, S. L. BRUNTON, J. L. PROCTOR, AND J. N. KUTZ, *Data-driven discovery of partial differential equations*, Science Advances, 3 (2017), p. e1602614.
 - [45] P. J. SCHMID, *Dynamic mode decomposition of numerical and experimental data*, Journal of fluid mechanics, 656 (2010), pp. 5–28.
 - [46] J. H. TU, C. W. ROWLEY, D. M. LUCHTENBURG, S. L. BRUNTON, AND J. N. KUTZ, *On dynamic mode*

- decomposition: Theory and applications*, arXiv preprint arXiv:1312.0041, (2013).
- [47] G. VALMORBIDA AND J. ANDERSON, *Region of attraction estimation using invariant sets and rational lyapunov functions*, *Automatica*, 75 (2017), pp. 37–45.
 - [48] D. VENTURI AND A. DEKTOR, *Spectral methods for nonlinear functionals and functional differential equations*, *Research in the Mathematical Sciences*, 8 (2021), pp. 1–39.
 - [49] M. O. WILLIAMS, M. S. HEMATI, S. T. DAWSON, I. G. KEVREKIDIS, AND C. W. ROWLEY, *Extending data-driven koopman analysis to actuated systems*, *IFAC-PapersOnLine*, 49 (2016), pp. 704–709.
 - [50] M. O. WILLIAMS, I. G. KEVREKIDIS, AND C. W. ROWLEY, *A data-driven approximation of the koopman operator: Extending dynamic mode decomposition*, *Journal of Nonlinear Science*, 25 (2015), pp. 1307–1346.
 - [51] M. O. WILLIAMS, C. W. ROWLEY, I. MEZIĆ, AND I. G. KEVREKIDIS, *Data fusion via intrinsic dynamic variables: An application of data-driven koopman spectral analysis*, *EPL (Europhysics Letters)*, 109 (2015), p. 40007.